

# Silicon katarometer with the BSC-type contacts

Jan M. Łysko, Joanna Łozinko, Jerzy Jaźwiński,  
Bogdan Latecki, Andrzej Panas, and Marianna Górską

Institute of Electron Technology, Al. Lotników 32/46, 02-668 Warszawa, POLAND

## ABSTRACT

Thermal conductivity detector (TCD, katarometer) silicon chip was designed with the BSC type (Back Side Contact) electrical contacts, covered by the Cr/Au layer. Detector consists of the two elements - glass plate and silicon chip. There are two flow channels formed at the glass-silicon interface - one for detection and the other for reference. Two highly symmetrical groups of resistors were aligned with the channels and, in the last stage of the fabrication sequence, released from the silicon substrate. Some of these resistors act as the heaters, the other ones as the detectors (thermoresistors) to detect changes of the flowing gas temperature. Tubing - gas inlets and outlets - was positioned at the detector edge, in the Si-glass interface plane. BSC-type electrical contacts application enabled very convenient bonding pads location. The Contacts formation process was optimized and integrated with the other technological steps.

**Keywords:** silicon, detector, katarometer, contacts

## 1. INTRODUCTION

Miniature, silicon Thermal Conductivity Detector (TCD, katarometer) is the element of the micro total analysis system ( $\mu$ TAS) under development in the IET, in cooperation with several academic institutions in Poland. It was designed and fabricated for measurements of gas mixtures compositions. Tests require only a few micro liters volume samples. A single sample is injected to the carrier gas stream (favorable helium) by the system of the silicon micro valves. It enters the capillary column where gas mixture is separated to the individual components <sup>1</sup> diluted in the carrier gas. Column outlet is connected with the detector inlet with the capillary and short tubing. Pure carrier gas flow through the parallel detector channel is used for reference. Changes of the gas temperature are detected by the system of sensitive thermoresistors and heaters located inside both detector channels. Comparison of the two electrical signals (typically Wheatstone bridge) gives the information about the gas chemical composition changes. With the fixed geometrical dimensions of the detector, and constant carrier gas flow rate and constant heating power delivered to the heater resistor, only three thermal parameters of the gas components affect the temperature profile along the flow channel. These parameters are: gas density, thermal capacity and thermal conductivity <sup>2</sup>.

## 2. DETECTOR DESIGN AND TECHNOLOGY

The detector consists of the two elements: silicon chip and glass plate, which are bonded together (anodic bonding or glue application). Silicon chip dimensions are: 15mm  $\times$  15mm  $\times$  0.39mm. It was fabricated with the application of the standard IC technology, with several non-standard technological steps, typical for the MEMS technology. Glass plate size is: 15mm  $\times$  15mm  $\times$  2mm. It was shaped with the precise mechanical processing – milling and dicing - of the glass wafer 3 inches in diameter and 2 mm thick. Silicon chip consists the two highly symmetrical sets of poly-Si resistor. One of them was suspended over the test channel, another one - over the reference channel. Every resistor has individual electrical outputs - through the contact windows in the SiO<sub>2</sub>/Si<sub>3</sub>N<sub>4</sub> layers (so-called buried contacts), to the n<sup>+</sup>-type diffusion paths doped by the phosphorous. These paths have connections to the BSC-type contacts and bonding pads located at the opposite side of the silicon chip. BSC-type contacts, buried contacts, poly-Si and n<sup>+</sup> paths total resistance is very small, less than 1  $\Omega$ . This can be neglected in the resistors performance of hundreds  $\Omega$ . Silicon wafers were diced into the individual chips with the standard diamond disk saw. At the end of the technological sequence detector silicon chips were etched in the TMAH + water solution. During this step grooves in the silicon chip were formed and resistors were under-etched to reduce resistors thermal capacity and power dissipation to the silicon substrate. Poly-Si resistor paths were suspended inside the detector flow channels. Mechanical release from the substrate support made them highly delicate and fragile. This imposed special requirements on the technological staff concerning chips manipulation, rinsing, drying, transport and storage procedure. After the silicon-glass attachment

step (with glue or anodic bonding) etched in the silicon chip and milled in the glass plate groves meet together and form the capillary flow channels at the silicon-glass interface. Fig. 1 illustrates arrangements of the resistors, channel and electrical connections on the mask layout.

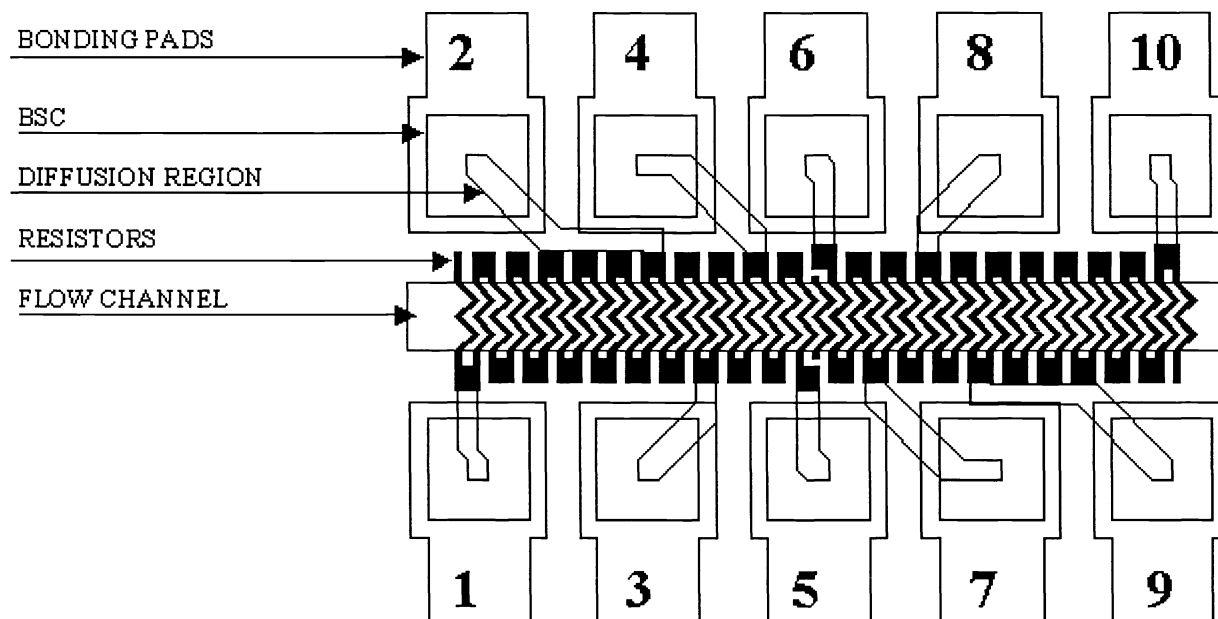


Fig. 1. Resistors arrangement on the detector chip

### 3. BSC-TYPE CONTACTS FORMATION

Electrical outputs from the poly-Si resistors consisted the BSC-type contacts. They were formed at the initial phase of the technological sequence. Formation of the BSC structures requires deep silicon substrate etching and heavy doping with phosphorous (very long time and high temperature). These could damage previously formed electronic elements. For the anisotropic etching of the mono crystalline (100) silicon substrate KOH+H<sub>2</sub>O 80°C solution and SiO<sub>2</sub>/Si<sub>3</sub>N<sub>4</sub> (1 μm / 0.1 μm) masking patterns were applied. Deep, square-footed pyramids grooves etching had to be precisely controlled and stopped when the remaining silicon membrane thickness reached the 20-30 μm range. Second photolithography mask aligned from the opposite side of the wafer, defined shapes of the diffusion paths in the dielectric masking layers. Deep phosphorous diffusion ( $x_j = 16 \mu\text{m}$ ) from the both sides of the wafers was carried out in the high temperature diffusion furnace. During this step  $n^+$  type regions in the p-type substrate were formed as the conductive paths and electrical contacts from one side of the wafer to another. Diffusion zones should meet in the middle of the silicon membranes ( $2 \cdot 16 \mu\text{m} > 30 \mu\text{m}$ ). Damaged layers were removed and new dielectric layers were deposited. Consecutive technological steps were focused on the poly-Si resistors formation: photolithography of buried contacts, poly-Si deposition and doping, photolithography of resistors with chemical etching, Si<sub>3</sub>N<sub>4</sub>/SiO<sub>2</sub> layers plasma deposition. Last phase of the technological sequence was associated to the bonding pads formation: dielectric layers removal from the BSC grooves, Cr/Au lift-off. These metal layers played dual role – as a good material for the bonding pads and as a silicon substrate inside the BSC grooves protection against the TMAH + water etching solution<sup>3</sup>. Wafers were diced into the individual chips and flow channel grooves were etched.

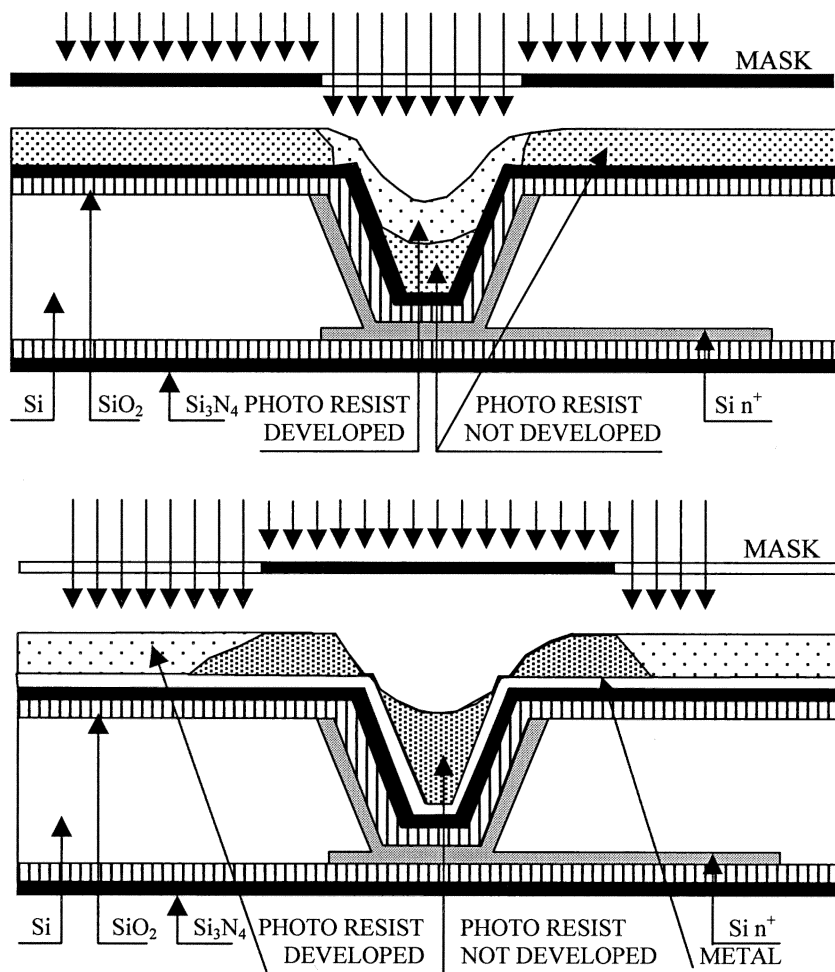


Fig. 2. Schematic cross-sections of the BSC type contacts.  
 Photolithography defects observed when the non-optimized resist was applied;  
 a) dielectric layers removal from the opening, b) metal layer formation inside the BSC

The BSC-type contacts formation required the photolithography steps optimization. Poor resist adhesion to the Si<sub>3</sub>N<sub>4</sub> layer, covering silicon wafer surface, required an additional SiO<sub>2</sub> thin layer deposition in the plasma reactor. High aspect ratio of the wafer surface caused difficulties with the conformal resist spin-on coverage and vacuum holders performance over the dominant part of the technological sequence. This required non-standard thick photo resists application. For the dielectric layers removal from the BSC grooves negative resist ma-N-1420 was applied. Exposition dose was 550 mJ/cm<sup>2</sup>. For the metal lift-off over the BSC grooves and bonding pads, positive resist ma-P-100 was applied. This time exposition dose was 400 mJ/cm<sup>2</sup>. Fig. 2a,b illustrate schematic cross sections and problems observed during the BSC-type contacts formation: excessive resist reminding after the development, not sufficient resist exposure inside the grooves and non continuities of the resist layer on the BSC edges. Fig. 3 illustrates SEM microphotography of the BSC-type contacts with the Cr/Au layers coverage, and filled by the conductive epoxy with the wire connection to the bonding pad.

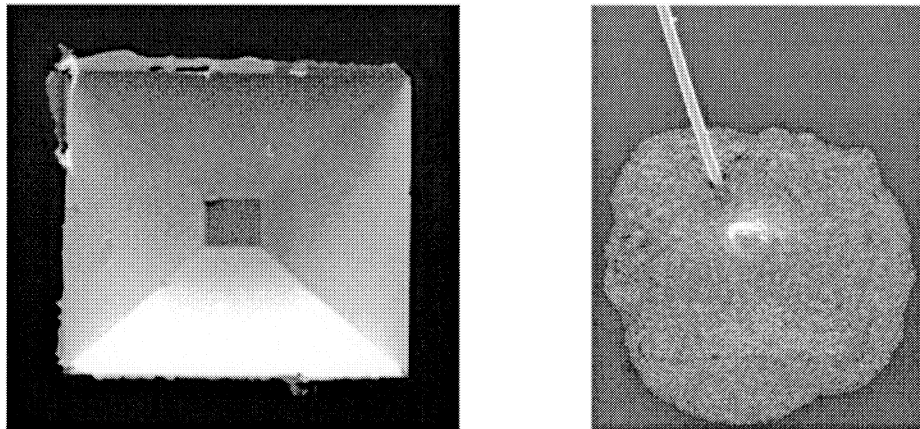


Fig. 3. BSC type contact SEM microphotography: on the left BSC covered by the Au/Cr, on the right: filled by the conductive epoxy, with the wire connection to the bonding pad

#### 4. RESULTS

The BSC-type contacts formation method was developed and optimized, accordingly to the katarometer design and technological sequence requirements. Problems associated to the photolithography on the high aspect ratio surfaces were solved by the non-standard, thick resists application and parameters optimization. TCD chips were placed in the packages (Fig. 4) and subjected to the functional tests. Experience obtained with the katarometer technology will be applied to the other silicon chemical sensors where the BSC-type contacts are desired, for instance gas sensors based on the  $\text{SnO}_2$ ,  $\text{ZnO}$  layers sensitivity or ISFET ion sensors.

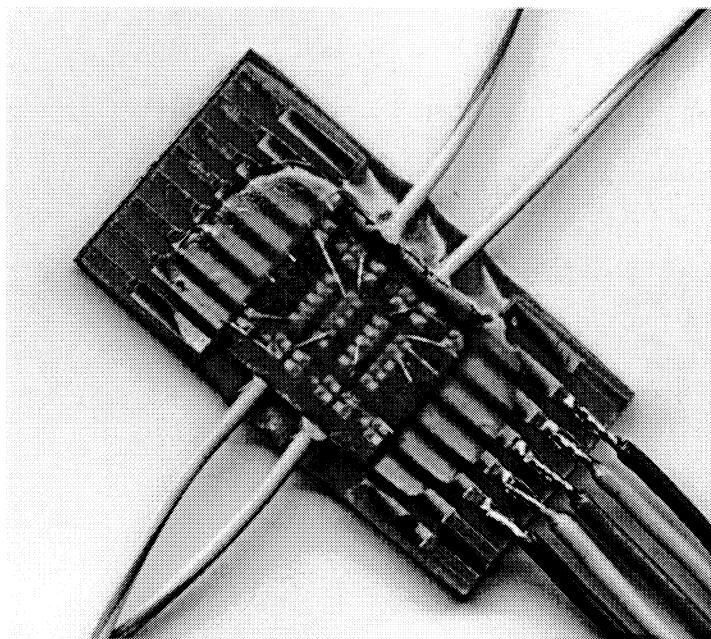


Fig. 4: TCD chip inside the package with the gas tubing and electrical outputs

## **5. ACKNOWLEDGEMENTS**

Publication sponsored by the Polish Committee for Scientific Research (KBN), grant no. PBZ 01915 : "Microsystems for the multi component gaseous media total analysis".

## **6. REFERENCES**

1. Dziuban J., Nieradko Ł., Górecka-Drzazga A., Mróz J., "Kapilarne mikrosystemy do całkowitej analizy mediów wieloskładnikowych", Elektronizacja 7-8'97, s.4-8, Elektronizacja 9'97, s.15-16.
2. Latecki B., Łozinko J., Łysko J.M., "Krzemowy katarometr – model analityczny", Elektronizacja 12/2001, s.23-25.
3. Zubel I., "The influence of atomic configuration of (h k l) planes on adsorption processes associated with anisotropic etching of silicon", Sensors and Actuators A 94 (2001) 76-86.